Weak-Interaction Rates in ^{16}O

W. C. Haxton
Department of Physics, FM-15, University of Washington, Seattle, Washington 98195

Calvin Johnson
W. K. Kellogg Radiation Laboratory, California Institute of Technology, Pasadena, California 91125
(Received 29 May 1990)

We describe a full nonspurious $4\hbar\omega$ shell-model calculation that successfully reproduces the low-lying spectrum of ^{16}O, including the superdeformed 0^+ (6.05 MeV) state, and discuss its connection with the coexistence model. This treatment provides a realistic microscopic framework for discussing various electroweak processes: $E2$ transitions in ^{16}O, the role of exchange currents and the pseudoscalar coupling constant in the $0^+ \leftrightarrow 0^-$ β-decay and μ-capture transition, and the evaluation of the Gamow-Teller inclusive response function.

PACS numbers: 21.60.Cs, 23.40.−s, 25.30.−c, 27.20.+n

Twenty years ago Brown and Green[1] developed a schematic coexistence model that demonstrated the importance of highly deformed four-particle–four-hole (4p4h) amplitudes (i.e., α-particle excitations) in the wave functions of low-lying even-J states in ^{16}O. The corresponding microscopic shell-model calculation requires a full $4\hbar\omega$ Hilbert space and has been considered a numerical challenge.[2] In this Letter we demonstrate that calculations of such complexity can now be performed,[3] including the evaluation of associated inclusive response functions. The principal motivation for this work is to improve our understanding of weak transition rates, particularly axial-charge transitions, in ^{16}O and neighboring nuclei. This is a key issue for interpreting parity-violation measurements in light nuclei such as ^{14}N, ^{18}F, and ^{19}F, for isolating the exchange-current contributions to the celebrated $0^+ \leftrightarrow 0^-$ β-decay and μ-capture transition in ^{16}O, and for testing the Goldberger-Treiman relation in nuclei. We also evaluate the Gamow-Teller (GT) distribution that governs the ^{16}O inclusive response to low-energy neutrinos.

In the work of Brown and Green (BG) the three lowest 0^+ states in ^{16}O were described as four valence nucleons occupying two $K=\frac{1}{2}$ orbitals in a deformed well, the analogs of the negative-parity No. 4 and positive parity No. 6 Nilsson orbitals. Three basis configurations were considered, the closed core, the 4p4h 0^+ excitation of that core, and one deformed 2p2h excitation of favored symmetry. The strong mixing of these configurations was attributed to the near degeneracy of the No. 4 and No. 6 orbitals for large positive deformation β, with the $2\hbar\omega$ interaction $V^{2\hbar\omega}$ then coupling the 0p0h and 2p2h configurations and the 2p2h and 4p4h configurations.

The BG model is simple and intuitive, yet successfully describes the low-lying spectrum and electromagnetic transition rates in ^{16}O. This model also provides perhaps our simplest example of a superdeformed state, the 0^+ level at 6.05 MeV. The appeal of the present work is the prospect of determining whether the BG model, including large nuclear deformation, emerges naturally from a microscopic calculation based on a realistic NN interaction (or, more correctly, the corresponding g matrix). In addition, because the $4\hbar\omega$ basis is complete for certain operators (unlike the coexistence model basis), inclusive response functions can be evaluated. We generate the full Gamow-Teller distribution by a moments method. The completeness of the $4\hbar\omega$ shell-model space is also important in permitting an exact projection of spurious center-of-mass excitations.

Many shell-model treatments of nuclei near $A=16$ have attempted to treat the physics of $V^{2\hbar\omega}$ by diagonalizing this interaction in a $2\hbar\omega$ Hilbert space. Such treatments cannot properly describe the 0_2^+ state, which BG identify as primarily 4p4h. First-order perturbation theory suggests that this approach may also fail to treat $2\hbar\omega$ excitations correctly: The $2\hbar\omega$ components of the Hilbert space interact with both the $0\hbar\omega$ and $4\hbar\omega$ components through $V^{2\hbar\omega}$. The problem is a subtle one: While the interaction between $2\hbar\omega$ and $4\hbar\omega$ components influences the energy eigenvalues of states that are primarily $2\hbar\omega$ in character, the absence of $4\hbar\omega$ components can be masked by adjusting splittings between p-shell and $2s\,1d$-shell single-particle energies. Yet, while the spectrum may appear superficially reasonable, one has, in effect, calculated the $0\hbar\omega$-$2\hbar\omega$ mixing starting with an incorrect $0\hbar\omega$ Hamiltonian, so that faulty wave functions may result.

Our diagonalization was performed in a full $4\hbar\omega$ Hilbert space (six oscillator shells are active), with an m-scheme representation for the basis states. We employed time-reversal and charge-conjugation symmetries to factor the Hamiltonian into four blocks corresponding to even and odd J and T, with each block containing about 86000 states. The extremum eigenvalues and corresponding eigenfunctions for each block were then deter-

mined by the Lanczos algorithm,[3] with about 270 iterations yielding full convergence for the ten lowest-energy states. In the spirit of BG, the strong interaction was only allowed to operate within the $1p$-$2s\,1d$ shells. (This choice also eliminates large $2\hbar\omega$ and $4\hbar\omega$ 1p1h amplitudes that could mix into the low-lying states only because the shell-model interaction does not properly respect the Hartree-Fock condition.) The adopted $0\hbar\omega$ Hamiltonian was formed from the Cohen and Kurath $1p$-shell interaction, the Brown and Wildenthal $2s\,1d$-shell interaction, and the Millener and Kurath cross-shell interaction, with the four single-particle energy splittings fitted to the isoscalar even-J states.[4] We used the bare Kuo g matrix for $V^{2\hbar\omega}$.[5] All configurations were allowed to interact through the center-of-mass Hamiltonian $H_{\text{c.m.}}$, and spurious components were removed by adding a large multiple of $H_{\text{c.m.}}$ to the potential described above. The same Hamiltonian was used in a $3\hbar\omega$ calculation of the negative-parity states.

The calculated and experimental isoscalar spectra of Fig. 1 are in very good agreement. We also show the spectrum that would result from diagonalizing H in a $2\hbar\omega$ model space. This illustrates the importance of the $2\hbar\omega$-$4\hbar\omega$ interaction in reducing the energy splitting between the ground state and those states that are primarily $2\hbar\omega$ in character (e.g., the 0_1^+-2_1^+ splitting is lowered by almost 8 MeV). The quality of the isovector spectrum is similar to that of Fig. 1, with the lowest five states in ^{16}F well reproduced. A low-lying 0^+1 state ($\sim$16 MeV) not seen experimentally is predicted. The

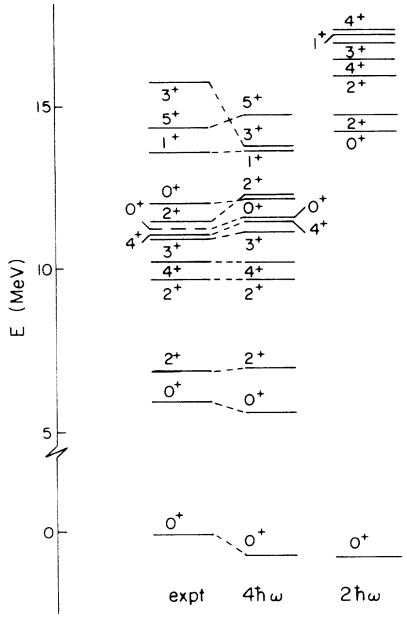

FIG. 1. A comparison of experiment and the $4\hbar\omega$ ^{16}O shell-model spectrum of $T=0$ states. The spectrum resulting from diagonalizing the same Hamiltonian in a $2\hbar\omega$ space is also shown.

isovector 0^-, 1^-,2^-,3^- group is also nicely reproduced. The principal difficulty with the isoscalar negative-parity spectrum is the failure to generate a second 1^-0 state near 9.59 MeV.

Table I shows the 0p0h, 2p2h, and 4p4h probabilities of the first 0^+ states in our calculation and in that of BG. (Note that the 0^+ 12.29-MeV state is the correct analog of the 0_3^+ BG state, since the nearby 0^+ state at 12.80 MeV is 73% 4p4h.) In the schematic model the 0p0h probability summed over the three 0^+ states must give 1, while in the shell model it mixes with the full set of 0^+ states in the $4\hbar\omega$ space. As the 0p0h fraction in the first three states is about 50%, the 2p2h and 4p4h shell-model fractions must be correspondingly larger. Despite this, the schematic and shell-model results are not too different: The correspondence for the 6.05-MeV state, which is primarily a 4p4h state, is very close, while both calculations conclude that about 70% of the strength in the 0_3^+ state is 2p2h.

The large intrinsic quadrupole moments that are postulated in the schematic model provide a simple explanation of the enhancements found in ^{16}O $E2$ transitions. We can now test whether this physics emerges from the shell-model and realistic NN interactions. As the shell model makes no explicit assumption about the single-particle basis, one must interpret the $E2$ transition density matrices in terms of suitable radial wave functions. We have used Ginocchio potential[6] wave functions, which are algebraic and yet closely resemble numerical finite-well wave functions (such as Woods-Saxon). The parameters of this potential were adjusted to reproduce the elastic (e,e') form-factor diffraction minimum and the height and location of the second diffraction maximum, as well as the $1p_{1/2}$ and $1p_{3/2}$ binding energies. The single-particle spherical shell model for ^{17}O produces an unbound $1d_{3/2}$ state, and in this respect does not provide an appropriate basis for interpreting transition density matrices between bound states. In a deformed well this problem need not arise, since the $d_{3/2}$ amplitudes could be sensibly associated with bound Nilsson orbitals. We avoid this complication by appealing to the schematic model, where the sd-shell excitations of ^{16}O involve a single bound Nilsson level (No. 6). This motivates our choice of a single binding energy for the sd-shell orbits in the Ginocchio well, which we take as the average of the shell-model $2s_{1/2}$, $1d_{5/2}$, and $1d_{3/2}$

TABLE I. Comparison of the shell-model (SM) and BG 0p0h, 2p2h, and 4p4h probabilities for the first three 0^+ states in ^{16}O.

	g.s.		0_2^+ (6.05 MeV)		0_3^+	
Probability	BG	SM	BG	SM	BG	SM
0p0h	0.76	0.42	0.07	0.04	0.17	0.03
2p2h	0.22	0.45	0.05	0.05	0.73	0.68
4p4h	0.02	0.13	0.88	0.90	0.10	0.30

TABLE II. Experimental, shell-model, and schematic-model ^{16}O $B(E2)$ values. (Gin. denotes the Ginocchio potential and h.o. the harmonic-oscillator wave function.)

Transition	Expt.	SM (Gin.)	SM (h.o.)	BG[a]
$2_1^+(6.92) \rightarrow 0_1^+(0.0)$	7.4 ± 0.2	4.3	1.4	5.3
$2_1^+(6.92) \rightarrow 0_2^+(6.05)$	65 ± 7	53	17	103
$2_2^+(9.84) \rightarrow 0_1^+(0.0)$	0.074 ± 0.007	0.054	0.12	
$2_2^+(9.84) \rightarrow 0_2^+(6.05)$	2.9 ± 0.7	0.68	1.3	
$2_3^+(11.52) \rightarrow 0_1^+(0.0)$	3.6 ± 1.2	2.2	0.65	3.3
$2_3^+(11.52) \rightarrow 0_2^+(6.05)$	7.4 ± 1.2	4.8	1.6	7.7
$4_1^+(10.36) \rightarrow 2_1^+(6.92)$	156 ± 14	63	20	152
$4_2^+(11.10) \rightarrow 2_1^+(6.92)$	2.4 ± 0.7	5.1	2.8	

[a]Reference 1.

binding energies, 2.2 MeV.

Experimental $B(E2)$ rates are compared to the shell-model and BG results in Table II. Also given are results for harmonic-oscillator wave functions (with an oscillator parameter $b=1.71$ fm chosen to reproduce the diffraction minimum of the elastic form factor). Bare charges are employed. The shell-model finite-well wave functions do quite well in reproducing experiment, almost as well as the schematic-model parametrization. Probably these results could be further improved by adjusting the *sd*-shell binding energy, but we have not attempted this. The harmonic-oscillator results are far less satisfactory.

The present study is a first step toward developing realistic shell-model treatments of parity nonconservation (PNC) in ^{14}N, ^{18}F, and ^{19}F. Adelberger and Haxton have argued that matrix elements of PNC and axial-charge operators depend delicately on 2p2h pairing correlations (because of the time-reversal properties of these operators), nuclear deformation, and a realistic treatment of the single-particle basis.[7] These are the criteria that defined our treatment of ^{16}O. Consequently, these wave functions should describe the well-studied $0^+ \leftrightarrow 0^-$ $^{16}\mathrm{O} \leftrightarrow {}^{16}\mathrm{N}$ μ-capture and β-decay transition. This transition is itself of great interest as a test of the enhancement of the axial-charge operator by two-body currents and of the strength of the pseudoscalar coupling constant F_P in nuclei.

The theoretical μ-capture and β-decay rates are[8]

$$\Gamma_\mu = \frac{G_F^2 \cos^2\theta_C}{2\pi} \frac{\varepsilon_\nu^2}{1+\varepsilon_\nu/M_f} F_A^2 |\bar{\phi}|^2 \delta_{\mathrm{NKO}}^{\mu} \times \left| \langle 0^- || \sum_{i=1}^{A} \left\{ j_0(qr_i)\boldsymbol{\sigma}(i)\cdot\frac{\boldsymbol{\nabla}(i)}{M} - \left[1+\frac{\varepsilon_\nu}{M}\left(1-m_\mu\frac{F_P}{F_A}\right)\right] j_1(qr_i)\boldsymbol{\sigma}(i)\cdot\hat{\mathbf{r}}(i) \right\} \tau_-(i) || 0^+ \rangle \right|^2, \tag{1a}$$

$$\Gamma_\beta = \frac{G_F^2 \cos^2\theta_C}{2\pi^3} F_A^2 \int d\varepsilon_e\, \varepsilon_e k_e (\omega_0 - \varepsilon_e)^2 F(Z,\varepsilon_e) \left| \langle 0^+ || \sum_{i=1}^{A} \left\{ \boldsymbol{\sigma}(i)\cdot\frac{\boldsymbol{\nabla}(i)}{M} - \delta_{\mathrm{NKO}}^{\beta}\frac{\omega_0}{3}\left(1+\frac{3\alpha Z}{2R\omega_0}\right)\boldsymbol{\sigma}(i)\cdot\mathbf{r}(i) \right\} \tau_+(i) || 0^- \rangle \right|^2, \tag{1b}$$

where M and M_f are the nucleon and nuclear masses, $|\bar{\phi}|^2$ is the muon probability at the nucleus, $F_A=1.26$ is the axial coupling, ε_ν and ε_e are the neutrino and electron energies, k_e is the electron momentum, $F(Z,\varepsilon_e)$ is the Dirac Coulomb correction, $R\sim 3.02$ is the nuclear radius, and ω_0 is the β-decay energy release. The lower component of the muon wave function and corrections of order ε_b/M, where ε_b is the muon binding energy, were ignored in deriving Eq. (1a); $\delta_{\mathrm{NKO}}^{\mu}\sim 0.88$ corrects for these omissions.[8] Similarly, $\delta_{\mathrm{NKO}}^{\beta}\sim 0.932$ represents the effect of using realistic atomic wave functions in the β-decay formula. In addition, the complete results contain a two-body axial-charge contribution that can be derived from a low-energy theorem based on PCAC (partial conservation of axial-vector current) and current algebra.[7,8] The corresponding matrix elements are evaluated from the shell-model two-body density matrix, modified by the correlation function used in Ref. 7.

The results of our shell-model–Ginocchio-potential calculations are

$$\Gamma_\mu = \begin{cases} 1.69\times 10^3 (1+0.040\alpha)^2\ \mathrm{sec}^{-1}, & (1+2)\text{-body}, \\ 1.18\times 10^3 (1+0.048\alpha)^2\ \mathrm{sec}^{-1}, & 1\text{-body}, \end{cases}$$

where $\alpha = m_\mu F_P/F_A - 7$ is the deviation of $m_\mu F_P/F_A$ from the PCAC value. A comparison to the experimental[9] value $\Gamma_\mu^{\mathrm{expt}} = 1560 \pm 94$ sec^{-1} yields $-0.26 < \alpha < -1.70$ for the full $(1+2)$-body calculation; that is, the $m_\mu F_P/F_A \sim 7$–9, a range near the PCAC value. The

corresponding β-decay results are

$$\Gamma_\beta = \begin{cases} 0.276\ \text{sec}^{-1}, & (1+2)\text{-body}, \\ 0.050\ \text{sec}^{-1}, & 1\text{-body}. \end{cases}$$

Three of the experimental determinations of Γ_β are in good agreement and yield $\Gamma_\beta^{\text{expt}} = 0.49 \pm 0.02\ \text{sec}^{-1}$.[9] In contrast to μ capture, a delicate cancellation occurs between the $\boldsymbol{\sigma}(i)\cdot\mathbf{V}(i)$ and $\boldsymbol{\sigma}(i)\cdot\mathbf{r}(i)$ β-decay operators, so that the effect of the exchange current is dramatic. However, the axial-charge operator two-body enhancement is insufficient to reproduce experiment. For comparison, an extreme $2s_{1/2}$-$1p_{1/2}$ single-particle model yields $\Gamma_\mu(\alpha=0) = 2.83\times10^3\ \text{sec}^{-1}$ and $\Gamma_\beta = 0.871\ \text{sec}^{-1}$ in a $(1+2)$-body calculation.

Often F_P is determined by fitting the ratio Γ_μ/Γ_β, which would then yield $m_\mu F_P/F_A \sim 14$, far from the PCAC value. This procedure, in effect, demands that theory predict incorrect values for both rates in order to reproduce the ratio. We think it far more plausible that the shell-model value for the magnitude of the axial-charge matrix element is slightly underestimated, while that for $\boldsymbol{\sigma}\cdot\mathbf{r}$ is slightly overestimated. Small adjustments ($\sim 15\%$) can yield the observed values of Γ_μ and Γ_β.

Another weak process of recent interest is the inclusive low-energy neutrino reaction $^{16}\text{O}(\nu_e, e^-)^{16}\text{F}$. This reaction is a potential background[10] in a proposed water Čerenkov detector precision measurement of the Weinberg angle. The allowed contribution to this cross section is governed by the $^{16}\text{F}/^{16}\text{N}$ $B(\text{GT})$ distribution, and work is underway to extract this distribution from forward-angle (p,n) measurements.[11] As our shell-model space is complete for the Gamow-Teller operator, we can predict the profile of this distribution, including the spreading effects of couplings to high-lying 2p2h and 4p4h 1^+1 states.

Inclusive response functions in very large Hilbert spaces can be efficiently evaluated with the Lanczos algorithm: For a given starting vector $|v\rangle$ the Jacobi matrix truncated after n interactions determines the $2n-1$ moments of $|v\rangle$ distributed over the energy eigenspectrum.[12] Using $|v\rangle = \sum_{i=1}^{A} \sigma_0 \tau_\pm(i)|\text{g.s.}\rangle$, this procedure quickly generates a very accurate $B(\text{GT})$ profile. The profile achieved after 290 iterations and including a Gaussian smoothing function of 1 MeV FWHM is shown in Fig. 2. The profile is fully converged. It will be interesting to see how well the spreading achieved in this very large Hilbert space reproduces experiment.

Also shown in Fig. 2 are the $B(\text{GT})$ results for a diagonalization of our Hamiltonian in a $2\hbar\omega$ Hilbert space. The resulting total $B(\text{GT})$ strength of 0.44 can be compared to the $4\hbar\omega$ value of 0.69. The two profiles differ more sharply at low excitation energies, where considerably more strength appears in the 4p4h calculation. However, the well-known discrepancy[13] between $2\hbar\omega$ shell-model calculations and experimental $B(\text{GT})$ strength below 7 MeV in ^{16}F is still not fully removed.

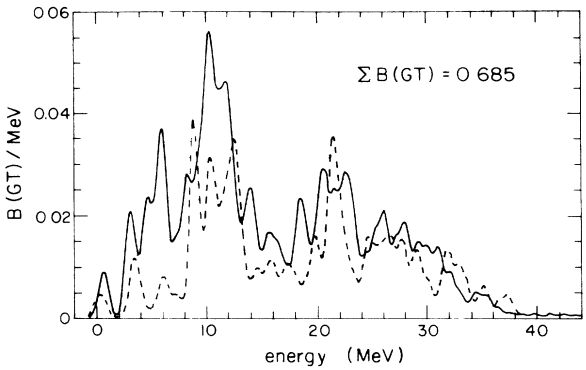

FIG. 2. The $4\hbar\omega$ (solid line) and $2\hbar\omega$ (dashed line) $B(\text{GT})$ spectra in ^{16}O. In each case excitation energies are measured relative to the lowest 1^+1 level.

More details of our calculations will be presented in a longer paper. We thank Val Zeps, Charles Hyde-Wright, and Kuniharu Kubodera for helpful discussions. This work was supported in part by the Department of Energy and the National Science Foundation. We thank the San Diego Supercomputer Center for providing CRAY X-MP time.

[1]G. E. Brown and A. M. Green, Nucl. Phys. **75**, 401 (1966).

[2]B. A. Brown and B. H. Wildenthal, Annu. Rev. Nucl. Part. Sci. **36**, 29 (1988).

[3]The code we employ is a revised version of that written by J. Dubach and W. Haxton, based on the Glasgow Lanczos shell-model program: R. R. Whitehead *et al.*, Adv. Nucl. Phys. **9**, 123 (1977). The code was adapted for the CRAY X-MP and the VaxStation 3200, the machines we used for the present calculations.

[4]The energy levels used in this fit correspond to the 0_2^+, 0_3^+, 2_1^+, 2_2^+, 4_1^+, and 4_2^+ states. The identification of the 0_3^+ state with a level at 11.26 MeV is controversial [F. Ajzenberg-Selove, Nucl. Phys. **A460**, 1 (1986)]. Its inclusion in the fit yields a slightly worse average rms deviation from experimental energies (51 vs 47 keV).

[5]T. T. S. Kuo (private communication).

[6]J. N. Ginocchio, Ann. Phys. (N.Y.) **152**, 203 (1984); **159**, 467 (1985).

[7]E. G. Adelberger and W. C. Haxton, Annu. Rev. Nucl. Part. Sci. **35**, 501 (1985).

[8]P. Guichon and C. Samour, Phys. Lett. **82B**, 28 (1979); S. Nozawa, K. Kubodera, and H. Ohtsubo, Nucl. Phys. **A453**, 645 (1986).

[9]I. S. Towner, Annu. Rev. Nucl. Part. Sci. **36**, 115 (1986), and references therein.

[10]W. C. Haxton, Phys. Rev. C **37**, 2660 (1988).

[11]J. Rapaport (private communication).

[12]R. R. Whitehead, in *Moment Methods in Many Fermion Systems* (Plenum, New York, 1980), p. 235.

[13]K. A. Snover *et al.*, Phys. Rev. C **27**, 1837 (1983).